Lattice vibrations in thin-film carbon: Electron–Rayleigh-wave interaction

Ko Sugihara
Center for Materials Science and Engineering, Massachusetts Institute of Technology, Cambridge, Massachusetts 02139
(Received 16 November 1987)

Sound-wave propagation in thin-film carbon is investigated in the long-wavelength approximation. The Rayleigh wave, with a small damping constant and with polarization along the c axis, has a small sound velocity $v_R \sim 10^4$ cm/sec if C_{44} is small. Since the Rayleigh-wave phonons interacting with carriers have small energies ($\hbar\omega/k_B \lesssim 1$ K), these phonons are highly excited even at helium temperature and they scatter carriers. Of particular interest for transport properties is the carrier relaxation time $\tau_R \sim 10^{-12}$ sec for film thickness $d \lesssim 100$ Å at $T \lesssim 1$ K. If the sample is assumed to be composed of an aggregate of many thin films, and each film weakly couples elastically with the others, the present theory is applicable to a sample with bulk thickness. The electron–Rayleigh-wave interaction is responsible for the unusual temperature dependence of the resistivity observed for a polyacrylonitrile-based fiber heat-treated to ~ 1300 °C. A comment is given about one possible mechanism for the anomalous linear temperature-dependent specific heat observed in some kinds of carbons and in polycrystalline graphite.

I. INTRODUCTION

The lattice dynamics for single-crystal graphite or highly oriented pyrolytic graphite (HOPG) has been extensively studied experimentally and theoretically.[1–7] The lattice properties of pregraphitic carbons are estimated from the corresponding properties for graphite by introducing the elastic constants for the pregraphitic carbons and/or by considering finite-size effects and crystallite orientation effects.

In this article it is pointed out that sound-wave propagation in thin-film carbons takes place in a different way from that in bulk graphite. If the sample is thin enough along the c axis (< 100 Å), the Rayleigh wave polarized along the c axis propagates with little damping and its sound velocity and frequency are given by $v_R \simeq (C_{44}/\rho_m)^{1/2}$ and $\omega \simeq v_R q$, where $q^2 = q_x^2 + q_y^2$ and ρ_m is the density of the sample. C_{44} is related to the shearing force and is very sensitive to crystal perfection, especially to the density of stacking faults. The magnitude of C_{44} thus ranges from 4.5×10^{10} dyn/cm^2 for a well-graphitized crystal[4,5] to 7×10^9 dyn/cm^2 for pregraphitic carbons with a high density of stacking faults.[8,9] A typical value of the Fermi wave vector k_F for the pregraphitic carbons, which are described by a two-dimensional band, is at most $\sim 10^6$ cm^{-1}. Accordingly, the energies of the Rayleigh-wave phonons interacting with the carriers are

$$\hbar\omega/k_B \simeq 0.4 \text{ K} , \tag{1.1}$$

where the values $C_{44} = 7\times10^9$ dyn/cm^2, $\rho_m = 2.26$ g/cm^3, and $q = 10^6$ cm^{-1} are employed. This implies that the Rayleigh-wave phonons interacting with carriers are highly excited even at ~ 1 K. This is a striking effect, and the carrier scattering rate by these phonons at ~ 1 K is comparable to the values of the phonon scattering rate in bulk graphite at ~ 50 K. This rate is proportional to d^{-2}, where d is the sample thickness. If the sample is assumed to be composed of an aggregation of many thin films and each film weakly couples elastically with the others, the present theory is applicable to a sample with bulk thickness.

In Sec. II the lattice vibrations of thin-film graphite are studied in the long-wavelength approximation, imposing boundary conditions on the sample surface. Two cases are studied: (i) the semi-infinite case and (ii) the thin-film case in Sec. III. The electron–Rayleigh-wave phonon interaction is treated in Sec. IV for the thin-film case and the carrier relaxation rate is calculated. This calculation is then applied to the anomalous temperature-dependent resistivity observed in polyacrylonitrile (PAN) fibers at low temperatures.[10,11] There is a brief discussion in Sec. V about one possible mechanism for the anomalous large linear temperature-dependent specific heat observed in some kinds of carbons and polycrystalline graphite.[12] The contribution from the Rayleigh-wave phonons is expected to be responsible for the specific-heat anomaly at low temperature. A summary is given in Sec. VI.

II. LATTICE DYNAMICS IN THIN-FILM CARBONS

The theory of the lattice vibrations in graphite was first proposed by Komatsu-Nagamiya and Komatsu[1] in connection with the low-temperature specific heat. The equations for the lattice vibrations are given by

$$\frac{\partial^2 u_n}{\partial t^2} = v_l^2 \frac{\partial^2 u_n}{\partial x^2} + v_t^2 \frac{\partial^2 u_n}{\partial y^2} + v_1^2 \left[\frac{1+\sigma}{2} \right] \frac{\partial^2 v_n}{\partial x \partial y} + \frac{\zeta}{c_0^2}(u_{n+1} + u_{n-1} - 2u_n) + \frac{\zeta}{2c_0} \left[\frac{\partial w_{n+1}}{\partial x} - \frac{\partial w_{n-1}}{\partial x} \right] , \tag{2.1a}$$

$$\frac{\partial^2 v_n}{\partial t^2}=v_l^2\frac{\partial^2 v_n}{\partial y^2}+v_t^2\frac{\partial^2 v_n}{\partial x^2}+v_l^2\left[\frac{1+\sigma}{2}\right]\frac{\partial^2 u_n}{\partial x\partial y}+\frac{\zeta}{c_0^2}(u_{n+1}+u_{n-1}-2u_n)+\frac{\zeta}{2c_0}\left[\frac{\partial w_{n+1}}{\partial y}-\frac{\partial w_{n-1}}{\partial y}\right], \tag{2.1b}$$

$$\frac{\partial^2 w_n}{\partial t^2}=-\kappa^2\Delta^2 w_n+\frac{v_z^2}{c_0^2}(w_{n+1}+w_{n-1}-2w_n)+\zeta\Delta w_n+\frac{\zeta}{2c_0}\left[\frac{\partial u_{n+1}}{\partial x}-\frac{\partial u_{n-1}}{\partial x}+\frac{\partial v_{n+1}}{\partial y}-\frac{\partial v_{n-1}}{\partial y}\right], \tag{2.1c}$$

where u_n, v_n, and w_n represent the displacement of a point (x,y) in the nth graphite layer. v_l and v_t are the longitudinal and transverse sound wave velocities associated with the in-plane vibration, v_z the sound velocity related to the out-of-plane vibration, σ the Poisson ratio given by C_{12}/C_{11}, c_0 the interlayer distance, and Δ is the two-dimensional Laplacian $\partial^2/\partial x^2+\partial^2/\partial y^2$, while κ^2 is a constant related to the bending modulus of the graphite layers and $\zeta=C_{44}/\rho_m$.[1,13]

In the long-wavelength approximation Eqs. (2.1a)–(2.1c) become

$$\frac{\partial^2 u}{\partial t^2}=v_l^2\frac{\partial^2 u}{\partial x^2}+v_t^2\frac{\partial^2 u}{\partial y^2}+v_l^2\left[\frac{1+\sigma}{2}\right]\frac{\partial^2 v}{\partial x\partial y}+\zeta\left[\frac{\partial^2 u}{\partial z^2}+\frac{\partial^2 w}{\partial x\partial z}\right], \tag{2.2a}$$

$$\frac{\partial^2 v}{\partial t^2}=v_l^2\frac{\partial^2 v}{\partial y^2}+v_t^2\frac{\partial^2 v}{\partial x^2}+v_l^2\left[\frac{1+\sigma}{2}\right]\frac{\partial^2 u}{\partial x\partial y}+\zeta\left[\frac{\partial^2 v}{\partial z^2}+\frac{\partial^2 w}{\partial y\partial z}\right], \tag{2.2b}$$

$$\frac{\partial^2 w}{\partial t^2}=-\kappa^2\Delta^2 w+v_z^2\frac{\partial^2 w}{\partial z^2}+\zeta\Delta w+\zeta\left[\frac{\partial^2 u}{\partial x\partial z}+\frac{\partial^2 v}{\partial y\partial z}\right]. \tag{2.2c}$$

As will be mentioned in Sec. V, the term $-\kappa^2\Delta^2 w$ in Eq. (2.2c) is responsible for the anomalous large linear temperature-dependent specific heat observed in some kinds of carbons and polycrystalline graphite.[12] However, this term is negligibly small compared with the other terms for $q\sim 10^6$ cm^{-1}, and can be neglected in calculating the electron–Rayleigh-wave interaction.

Solutions for Eqs. (2.2a)–(2.2c) are assumed in the form

$$\begin{bmatrix}u\\v\\w\end{bmatrix}=\begin{bmatrix}U\\V\\W\end{bmatrix}\exp[\lambda z+i(q_x x+q_y y-\omega t)]\,. \tag{2.3}$$

Inserting Eq. (2.3) into Eqs. (2.2a)–(2.2c), we obtain

$$M\begin{bmatrix}U\\V\\W\end{bmatrix}=0\,, \tag{2.4}$$

where

$$M=\begin{bmatrix}\omega^2+\zeta\lambda^2-v_l^2q_x^2-v_t^2q_y^2 & -v_l^2\left[\frac{1+\sigma}{2}\right]q_xq_y & i\zeta\lambda q_x\\ -v_l^2\left[\frac{1+\sigma}{2}\right]q_xq_y & \omega^2+\zeta\lambda^2-v_l^2q_y^2-v_t^2q_x^2 & i\zeta\lambda q_y\\ i\zeta\lambda q_x & i\zeta\lambda q_y & \omega^2+v_z^2\lambda^2-\zeta q^2\end{bmatrix}. \tag{2.5}$$

By introducing the transformation matrix:

$$T=\begin{bmatrix}n_x & n_y & 0\\ -n_y & n_x & 0\\ 0 & 0 & 1\end{bmatrix},\quad n_x=q_x/q,\ n_y=q_y/q\,, \tag{2.6}$$

the transformed matrix $\tilde{M}=TMT^{-1}$ becomes

$$\tilde{M}=\begin{bmatrix}\omega^2+\zeta\lambda^2-v_l^2q^2 & 0 & i\zeta\lambda q\\ 0 & \omega^2+\zeta\lambda^2-v_t^2q^2 & 0\\ i\zeta\lambda q & 0 & \omega^2+v_z^2\lambda^2-\zeta q^2\end{bmatrix}. \tag{2.7}$$

The secular equation $\det\tilde{M}=0$ yields the algebraic equation

$$(\omega^2+\zeta\lambda^2-v_t^2q^2)[(\omega^2+\zeta\lambda^2-v_l^2q^2)(\omega^2+v_z^2\lambda^2-\zeta q^2)+\zeta^2\lambda^2q^2]=0\,. \tag{2.8}$$

Equation (2.8) implies that only the longitudinal in-plane vibration couples with the out-of-plane vibration. The same situation is realized in the bulk sample.[1]

The sample is bounded at $z=0$ and $z=-d$ along the c axis, and its extension in the xy-plane is assumed to be infinite. To solve Eq. (2.4), two limiting boundary conditions are imposed at $z=0$ and $z=-d$: (i) the strain-free condition $e_{xz}=e_{yz}=e_{zz}=0$; (ii) the stress-free condition $T_{xz}=T_{yz}=T_{zz}=0$. Both boundary conditions give rise to the same equations:

$$\frac{\partial u}{\partial z}+\frac{\partial w}{\partial x}=0, \quad \frac{\partial v}{\partial z}+\frac{\partial w}{\partial y}=0, \quad \frac{\partial w}{\partial z}=0 , \tag{2.9}$$

at $z=0$ and $z=-d$. It is easily shown that the Rayleigh wave propagation (λ real) does not take place in the uncoupled mode which corresponds to the in-plane transverse vibration. Namely, we have

$$\omega^2=\zeta q_z^2+v_t^2 q^2 \text{ and } \lambda=iq_z . \tag{2.10}$$

To obtain solutions for the Rayleigh-wave propagation, Eq. (2.3) is assumed to be in the form

$$\begin{bmatrix} u \\ v \\ w \end{bmatrix}=\begin{bmatrix} U \\ V \\ W \end{bmatrix}\exp[\lambda z+i(qx-\omega t)] . \tag{2.11}$$

Equation (2.11) does not lack generality. Substituting Eq. (2.11) into Eq. (2.2b), we obtain

$$v=0 , \tag{2.12}$$

and Eq. (2.4) becomes

$$\begin{aligned} &(\omega^2+\zeta\lambda^2-v_l^2q^2)U+i\zeta\lambda qW=0 , \\ &i\zeta\lambda qU+(\omega^2+v_z^2\lambda^2-\zeta q^2)W=0 . \end{aligned} \tag{2.13}$$

Two positive roots λ_1^2 and λ_2^2 exist, if the Rayleigh-wave velocity $v_R=\omega/q$ satisfies the condition

$$v_R^2<\zeta , \tag{2.14}$$

and the displacement vector $(u,0,w)$ becomes

$$\begin{aligned} u=&[i\alpha(Ae^{\alpha qz}+Ce^{-\alpha qz}) \\ &+i\beta(Be^{\beta qz}+De^{-\beta qz})]e^{i(qx-\omega t)} , \\ w=&[\gamma(Ae^{\alpha qz}-Ce^{-\alpha qz}) \\ &+\delta(Be^{\beta qz}-De^{-\beta qz})]e^{i(qx-\omega t)} , \end{aligned} \tag{2.15}$$

where $(\lambda_1/q)^2=\alpha^2$, $(\lambda_2/q)^2=\beta^2$. The coefficients α, β, γ, and δ are complicated functions of v_l, v_z, and ζ, while A, B, C, D and v_R are determined from the boundary conditions given by Eq. (2.9). To estimate α, β, γ, and δ, the following set of parameters is employed:[4,5,8]

$$\begin{aligned} &v_l=(C_{11}/\rho_m)^{1/2}=2.10\times10^6 \text{ cm/sec} , \\ &\rho_m=2.26 \text{ g/cm}^3 , \\ &v_t=[(C_{11}-C_{12})/2\rho_m]^{1/2}=1.39\times10^6 \text{ cm/sec} , \\ &v_z=(C_{33}/\rho_m)^{1/2}=4.0\times10^5 \text{ cm/sec} , \\ &C_{44}=4.5\times10^{10} \text{ to } 0.7\times10^{10} \text{ dyn/cm}^2 . \end{aligned} \tag{2.16}$$

C_{44} (or ζ) is very sensitive to crystal perfection, especially to the density of stacking faults,[8] while C_{33} is approximately independent of crystal perfection. From Eq. (2.16) we have

$$\begin{aligned} &\alpha\simeq v_l/\zeta^{1/2}=33.3 , \\ &\beta\simeq(\zeta-v_R^2)^{1/2}/v_z<\zeta^{1/2}/v_z=0.16 , \\ &\gamma\simeq\zeta/v_z^2=0.025 , \\ &\delta\simeq v_l^2/\zeta\simeq\alpha^2 , \end{aligned} \tag{2.17}$$

where $\zeta=0.40\times10^{10}$ cm^2/sec^2, which is a typical value for pregraphitic carbons with a high density of stacking faults.[8,14]

By inserting the displacement vector $(u,0,w)$ given by Eq. (2.15) into the boundary condition Eq. (2.9) and by eliminating A, B, C, and D, we obtain the following condition:

$$(\beta-\beta_0)(e^{2\alpha qd}-1)(e^{2\beta qd}-1)-4\beta\beta_0(e^{\alpha qd}-e^{\beta qd})^2=0 , \tag{2.18}$$

where

$$\beta_0\simeq\alpha\gamma/\delta\simeq\zeta^{3/2}/v_l v_z^2=7.53\times10^{-4} . \tag{2.19}$$

III. RAYLEIGH-WAVE PROPAGATION

In the following we consider two cases: (i) the semi-infinite case $d=\infty$, and (ii) the thin-film case with $qd\lesssim1$.

(i) $d=\infty$: *the semi-infinite case.* In this limit, Eq. (2.18) leads to $\beta=\beta_0$. Then, we have

$$v_R\simeq(\zeta-\beta_0^2v_z^2)^{1/2}\simeq\zeta^{1/2}=6.3\times10^4 \text{ cm/sec} , \tag{3.1}$$

and

$$v_R/v_l\simeq\zeta^{1/2}/v_l=\tfrac{1}{30}\ll1 . \tag{3.2}$$

In this case the terms including $e^{-\alpha qz}$ and $e^{-\beta qz}$ in Eq. (2.15) disappear, and u and w become

$$\begin{aligned} u&=iA(\alpha e^{\alpha qz}-\beta_0 e^{\beta_0 qz})e^{i(qx-\omega t)} , \\ w&=\alpha A(\beta_0 e^{\alpha qz}-\alpha e^{\beta_0 qz})e^{i(qx-\omega t)} . \end{aligned} \tag{3.3}$$

Equation (3.3) approximately satisfies the boundary condition Eq. (2.9), since $\beta_0/\alpha\simeq2\times10^{-5}$.

As is shown in Eq. (3.3), u and w are composed of two different terms: one is a rapidly damping term with $e^{\alpha qz}$ and the other is a slowly damping wave with $e^{\beta_0 qz}$. This situation reflects the highly anisotropic elastic properties in graphite:

$$v_l^2\gg v_z^2\gg\zeta . \tag{3.4}$$

The above results are easily extended to the case with a wave vector $\mathbf{q}=(q_x,q_y)$. In terms of the phonon operators, Eq. (3.3) is rewritten as

$$\begin{aligned} \begin{bmatrix} u \\ v \end{bmatrix}=&i\sum_{\mathbf{q}}\frac{\mathbf{q}}{q}B_q(\alpha e^{\alpha qz}-\beta_0 e^{\beta_0 qz}) \\ &\times(b_q^\dagger e^{-i(\mathbf{q}\cdot\mathbf{r}-\omega t)}-b_q e^{i(\mathbf{q}\cdot\mathbf{r}-\omega t)}) , \end{aligned} \tag{3.5}$$

and

$$\mathbf{w}=\alpha\mathbf{n}\sum_{\mathbf{q}}B_q(\beta_0 e^{\alpha qz}-\alpha e^{\beta_0 qz})\times(b_q^\dagger e^{-i(\mathbf{q}\cdot\mathbf{r}-\omega t)}+b_q e^{i(\mathbf{q}\cdot\mathbf{r}-\omega t)}) , \tag{3.6}$$

where $\mathbf{n}=(0,0,1)$, and $b_q^\dagger$ and b_q denote the phonon operators. B_q is determined by the condition

$$2\int dr\frac{\rho_m}{2}(|\dot{u}|^2+|\dot{v}|^2+|\dot{w}|^2)=\sum_{\mathbf{q}}\hbar\omega_q(b_q^\dagger b_q+\tfrac{1}{2}) . \tag{3.7}$$

Then, we have

$$B_q\simeq\left[\frac{\hbar}{\rho_m v_R S}\frac{\beta_0}{\alpha^4}\right]^{1/2} , \tag{3.8}$$

where S is the surface area of the sample.

(ii) *d finite: the thin-film case.* It is not easy to obtain an expression for v_R in the general case with an arbitrary qd value. However, it is possible to solve for v_R if the conditions of $\beta qd\ll 1$ and $qd\lesssim 1$ are satisfied. By using the conditions $\alpha qd\gg 1\gg\beta qd$ and $qd\lesssim 1$, Eqs. (2.17) and (2.18) yield

$$v_R^2\simeq\zeta-\frac{2\beta_0 v_z^2}{qd}\simeq\zeta,\quad \beta=\left[\frac{2\beta_0}{qd}\right]^{1/2} . \tag{3.9}$$

$v_R\simeq\zeta^{1/2}$ is the same as the value for $d=\infty$. Therefore, in samples with a high density of stacking faults (small ζ or C_{44}), the Rayleigh wave propagates with a small sound velocity which is much smaller than $v_z=4.0\times10^5$ cm/sec. The displacements u and w are given by

$$\begin{aligned} u&\simeq iA(\alpha e^{\alpha qz}-\alpha e^{-\alpha q(z+d)}\\ &\quad-\beta_0\cosh\beta qz-\beta\sinh\beta qz)e^{i(qx-\omega t)} ,\\ w&\simeq\alpha A[\beta_0 e^{\alpha qz}-\beta_0 e^{-\alpha q(z+d)}\\ &\quad-\alpha\cosh\beta qz-(\alpha\beta_0/\beta)\sinh\beta qz]e^{i(qx-\omega t)} . \end{aligned} \tag{3.10}$$

The first and second terms in parentheses in Eqs. (3.10) represent rapidly damped waves and the third and fourth terms are very weakly damped. In terms of the phonon operators $b_q^\dagger$ and b_q, the displacement vectors are given by

$$\begin{aligned} \begin{bmatrix}u\\ v\end{bmatrix}&\simeq i\sum_{\mathbf{q}}\frac{\mathbf{q}}{q}B_q(\alpha e^{\alpha qz}-\alpha e^{-\alpha q(z+d)}\\ &\quad-\beta_0\cosh\beta qz-\beta\sinh\beta qz)\\ &\quad\times(b_q^\dagger e^{-i(\mathbf{q}\cdot\mathbf{r}-\omega t)}-b_q e^{i(\mathbf{q}\cdot\mathbf{r}-\omega t)}) , \end{aligned} \tag{3.11}$$

$$\begin{aligned} \mathbf{w}&\simeq\alpha\mathbf{n}\sum_{\mathbf{q}}B_q[\beta_0 e^{\alpha qz}-\beta_0 e^{-\alpha q(z+d)}\\ &\quad-\alpha\cosh\beta qz-(\alpha\beta_0/\beta)\sinh\beta qz]\\ &\quad\times(b_q^\dagger e^{-i(\mathbf{q}\cdot\mathbf{r}-\omega t)}+b_q e^{i(\mathbf{q}\cdot\mathbf{r}-\omega t)}) , \end{aligned} \tag{3.12}$$

where $\mathbf{q}=(q_x,q_y,0)$ and $\mathbf{n}=(0,0,1)$. It would appear that Eqs. (3.11) and (3.12) do not seem to be symmetrical around $z=-d/2$. However, this is not the case, since (u,v,w) are approximately symmetric around $z=-d/2$ because of the condition $\beta qd\ll 1$. Inspection of Eqs. (3.11) and (3.12) therefore yields

$$u,v\ll w\simeq-\alpha^2\sum_{\mathbf{q}}B_q\cosh\beta qz[b_q^\dagger e^{-i(\mathbf{q}\cdot\mathbf{r}-\omega t)}+b_q e^{i(\mathbf{q}\cdot\mathbf{r}-\omega t)}] , \tag{3.13}$$

then, we obtain

$$B_q\simeq\frac{1}{\alpha^2}\left[\frac{\hbar}{2\rho_m\omega_q\Omega}\right]^{1/2} , \tag{3.14}$$

where Ω is the sample volume.

IV. ELECTRON–RAYLEIGH-WAVE INTERACTION

The electron–Rayleigh-wave phonon interaction is calculated according to the procedure employed by Sugihara and Sato[15] in the study of the electrical conductivity of graphite.

If we assume that the ions are displaced without being deformed, the perturbing potential is given by

$$\mathcal{H}'=-\sum_{j,\mu}\xi_{j\mu}\mathrm{grad}U_{j\mu} , \tag{4.1}$$

where

$$\xi_{j\mu}=(u(\mathbf{R}_{j\mu}),v(\mathbf{R}_{j\mu}),w(\mathbf{R}_{j\mu})),\quad U_{j\mu}=U(\mathbf{r}-\mathbf{R}_{j\mu}) . \tag{4.2}$$

Here, j represents the jth unit cell and μ the nonequivalent carbon atoms in the unit cell. $U_{j\mu}$ is the potential energy of an electron due to the ion (j,μ). In the present problem

$$w\gg u,v \tag{4.3}$$

and

$$w(R)\simeq-\alpha^2\sum_{\mathbf{q}}B_q\cosh\beta qz(b_q^\dagger e^{-i(\mathbf{q}\cdot\mathbf{r}-\omega t)}+b_q e^{i(\mathbf{q}\cdot\mathbf{r}-\omega t)}) , \tag{4.4}$$

where $\mathbf{R}=(\mathbf{r},z)$ [see Eq. (3.13)]. The matrix elements of $\mathcal{H}'$ are proportional to the following type of integral:

$$\int\Psi_{t',k'}^*\left[\sum_{j,\mu}e^{\pm i\mathbf{q}\cdot\mathbf{R}_{j\mu}}e^{\beta qz_{j\mu}}\mathbf{n}_q\mathrm{grad}U_{j\mu}\right]\Psi_{t,k}d\mathbf{r} , \tag{4.5}$$

where t and t' are suffixes specifying electron and hole states and $\mathbf{q}=(q_x,q_y,0)$, $\mathbf{n}_q=(0,0,1)$. The expression (4.5) then becomes[15]

$$\frac{1}{d}\frac{-i\mathbf{n}_q\cdot(\mathbf{k}-\mathbf{k}')}{\beta q+i(k_z-k_z')}D\delta_{\mathbf{k}_a-\mathbf{k}_a',\pm\mathbf{q}} , \tag{4.6}$$

where $\mathbf{k}_a=(k_x,k_y,0)$ and $\mathbf{k}=(\mathbf{k}_a,k_z)$. Here D is the electron-phonon interaction associated with the out-of-plane vibration in bulk graphite and was estimated to be[16]

$$D=3.7\text{ eV} . \tag{4.7}$$

From Eq. (3.9) we have

$$\beta q \sim 10^4 \text{ cm}^{-1} , \tag{4.8}$$

for $d \simeq 10$ Å and $q \simeq 10^6$ cm^{-1}. This value is much smaller than $k_z - k_z'$ except for the special case $k_z - k_z' \simeq 0$; then the expression (4.6) becomes

$$-\frac{iD}{d}\delta_{k_a - k_a', \pm q} . \tag{4.9}$$

Thus, the relaxation rate due to the scattering by the Rayleigh-wave phonons is obtained as follows:

$$\frac{1}{\tau_R(E_k)} \simeq \frac{2\pi k_B T D^2}{\hbar \rho_m v_R^2 d^2 \Omega} \sum_{k'} \frac{1}{q^2}\left[1 - \frac{k_x'}{k_x}\right]\delta(E_k - E_{k'}) , \tag{4.10}$$

where the high-temperature approximation for phonons

$$N_q \simeq N_q + 1 \simeq k_B T/\hbar\omega_q , \tag{4.11}$$

is employed, since typical energies for the Rayleigh-wave phonons which interact with carriers are

$$\hbar\omega_q/k_B = \hbar v_R q/k_B \simeq 4.8\times 10^{-7} q < 1 \text{ K} , \tag{4.12}$$

for $q \lesssim 10^6$ cm^{-1}. From Eqs. (4.10) and (4.11) we obtain

$$\frac{1}{\tau_R(E)} \simeq \frac{k_B T}{4\hbar\rho_m c_0}\left[\frac{1}{E}\right]\left[\frac{D}{v_R d}\right]^2 , \tag{4.13}$$

where c_0 denotes the interlayer spacing. In deriving Eq. (4.13) the two-dimensional dispersion $E = p_0 k_a$ where $p_0 = (3^{1/2}/2)\gamma_0 a$ is employed. Inserting

$$D = 3.7 \text{ eV}, \quad \rho_m = 2.26 \text{ g/cm}^3, \quad c_0 = 3.35 \text{ Å} , \tag{4.14}$$

$$E = 0.01 \text{ eV}, \quad v_R = 6.3\times 10^4 \text{ cm/sec}, \quad d = 70 \text{ Å} ,$$

into Eq. (4.13), one obtains

$$\frac{1}{\tau_R} \simeq 4.8\times 10^{11} \text{ T/sec K} . \tag{4.15}$$

It should be noted that $1/\tau_R$ at $T = 1$ K is comparable to the scattering rate due to phonons in single-crystal graphite at $T \sim 50$ K.[16] Thus, the Rayleigh-wave interaction produces a striking effect, and this effect is expected to be responsible for the unusual low-temperature electrical resistivity behavior of PAN-based fibers,[10,11] which is shown in Figs. 1(a) and 1(b). At low temperatures the resistivity increases with temperature and exhibits a maximum between 30 and 35 K. The resistivity decrease above $T_{\max}$ is ascribed to an increase in carrier density. It is unusual that the resistivity has a significant temperature dependence even at liquid-helium temperature. From Figs. 1(a) and 1(b) we have that the ratio

$$\frac{R(20 \text{ K}) - R(10 \text{ K})}{R(T=0)} \simeq \text{a few percent} . \tag{4.16}$$

This magnitude is expected if the relaxation rate associated with the residual resistance $R(T=0)$ has a value

$$(1/\tau)_{\text{residual}} \sim 10^{14} \text{ sec}^{-1} , \tag{4.17}$$

which is not an unreasonable value for pregraphitic carbons. The decrease of $dR(T)/dT$ with increasing temperature below $T_{\max}$ is due to an increase in carrier density. Since the Fermi energy for these samples is low, an increase in carrier concentration is expected below ~ 30 K. The carrier density increase above $T_{\max}$ is a dominant

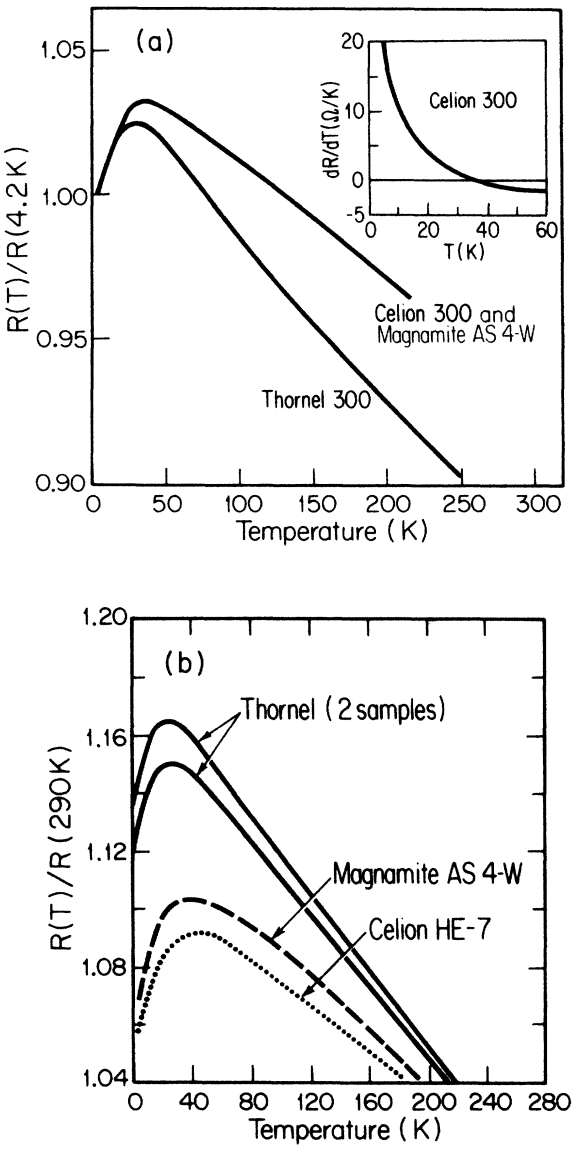

FIG. 1. (a) The variation with temperature of the reduced resistivity of carbon fibers. The inset shows the temperature dependence dR/dT below 50 K. Celion 300 is a PAN-based fiber with heat-treatment temperature (HTT) ~ 1300°C. PAN-based fibers manufactured by Hercules Powder Co. (Magnamite AS 4-W) and one from Union Carbide Corp. (Thornel 300) exhibit a similar behavior (Ref. 10). (b) The variation of reduced resistance $R(T)/R(290 \text{ K})$ for several PAN-based fibers with HTT ~ 1300°C. The resistance continues to fall with increasing slope down to the lowest measurement temperature (~ 1.5 K) (Ref. 11).

factor which controls the temperature dependence of the resistivity [see Figs. 1(a) and 1(b)].

The electron–Rayleigh-wave interaction is also responsible for the temperature-dependent negative magnetoresistance of pregraphitic carbons at low temperatures.[17,18] This will be treated in a separate paper. Another interesting effect in which the Raleigh wave may play an important role is the specific-heat anomaly in disordered carbons.[12] This is briefly discussed in the next section.

V. A COMMENT ON THE ANOMALOUS LINEAR TEMPERATURE-DEPENDENT SPECIFIC HEAT IN CARBONS

Some kinds of disordered carbons exhibit an anomalous, large linear temperature-dependent specific heat which cannot be ascribed to the carrier contribution.[12] To consider this problem, it is necessary to take into account the $-\kappa^2\Delta^2 w$ term in Eq. (2.2c), which is neglected in the previous sections. However, its contribution to the specific heat is important since the relevant wave vector is not restricted to small values of $q \sim 10^6\ \mathrm{cm}^{-1}$ in considering the contribution from the phonon degrees of freedom. Introduction of the $-\kappa^2\Delta^2 w$ term provides an extra contribution $\kappa^2 q^4$ to ω^2 and the Rayleigh wave then has a dispersion relation

$$\omega^2=\kappa^2 q^4+v_R^2 q^2 . \tag{5.1}$$

It should be noted that the most important contribution to ω^2 for bulk samples is $v_z^2 q_z^2$, though this term does not appear in thin film samples, as was discussed in the previous sections. Since κ has a value of $\sim 6\times 10^{-3}$ $\mathrm{cm}^2/\mathrm{sec}$,[1,2] the $\kappa^2 q^4$ term exceeds the $v_R^2 q^2$ term for $q \lesssim 10^7\ \mathrm{cm}^{-1}$. If the $v_R^2 q^2$ term is neglected in Eq. (5.1), we obtain a linear temperature-dependent specific heat at low temperatures:

$$C_R=\frac{d}{dT}U_R ,$$

$$U_R=\sum_q \frac{\hbar\omega_q}{\exp(\hbar\omega_q/k_B T)-1}\simeq\frac{(k_B T)^2 G(z_{\max})}{4\pi\hbar c_0\kappa} , \tag{5.2}$$

where

$$G(z)=\int_0^z dx\frac{x}{e^x-1},\quad z_{\max}=\hbar\kappa q_{\max}^2/k_B T , \tag{5.3}$$

and c_0 is the interlayer distance. Equation (5.2) is valid for $T>3$ K. Since we are interested in the specific heat at liquid-helium temperature,[12] $z_{\max}$ can be replaced by infinity and we have

$$C_R=\gamma_R T,\quad \gamma_R=\frac{k_B^2 G(\infty)}{2\pi\hbar c_0\kappa},\quad G(\infty)=\frac{\pi^2}{6} . \tag{5.4}$$

Typical examples for the anomalous specific heat are shown in Figs. 2(a) and 2(b).[12] The sharp peak observed below 1 K is ascribed to localized spin centers which give rise to an extra ESR absorption.[12] Apart from this contribution C/T is expressed by

$$C/T=\alpha T^2+\gamma , \tag{5.5}$$

where the αT^2 term is the normal Debye specific-heat contribution. The increase in α with decreasing heat-treatment temperature (HTT) is related to a decrease in rigidity and characteristic vibrational frequency, which are reflected in an increased room-temperature specific heat.[12] The electronic contribution to the specific heat in graphite is[9]

$$\gamma_{\mathrm{el}}=0.0138\ \mathrm{mJ/mol\,K^2} , \tag{5.6}$$

while the observed linear temperature-dependent specific heat in pregraphitic carbons and in polycrystalline graphites provides[12]

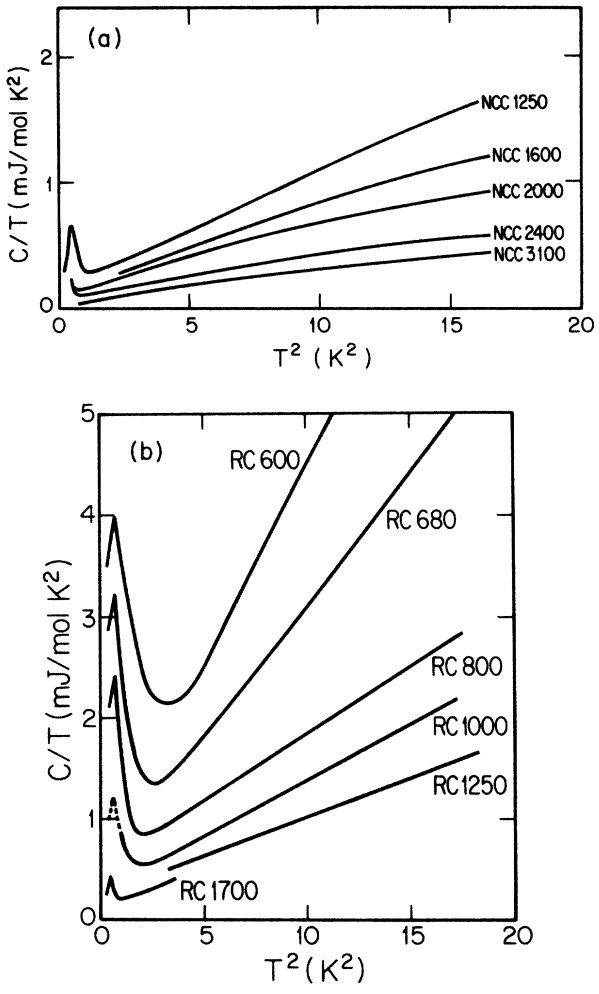

FIG. 2. (a) Specific-heat curve obtained for various heat-treated National Carbon Company baked carbon rods (NCC) as reported by Delhaes and Hishiyama (Ref. 19) (The number indicates the HTT.) The curve for NCC 1250 is added for completeness (Ref. 20). The curve for NCC 3100 agrees well with the data of Keesom and Pearlman (Ref. 21) for polycrystalline graphite (Ref. 12). (b) Specific-heat curves obtained for various heat-treated, laboratory-made raw coke rods (needle coke made from Resin C coal tar pitch with Resin C binder) (Refs. 12, 22, and 23).

$$\gamma \simeq 10^3 - 10^2 \ \mu J/\text{mol K}^2 , \tag{5.7}$$

which is one or two orders of magnitude larger than γ_{el} [see Figs. 2(a) and 2(b)]. Inserting $c_0 = 3.4$ Å and $\kappa = 6 \times 10^{-3}$ cm^2/sec into Eq. (5.4), we obtain

$$\frac{\gamma_R}{\gamma_{el}} = 3 \times 10^2 , \tag{5.8}$$

which is consistent with the observed results. The decrease of the value of γ with HTT is consistent with the present model. The film thickness d which specifies the elastically correlated length along the c axis increases with HTT and in the samples with large d the distance through which the Rayleigh wave propagates without damping is much smaller than d. In these samples the contribution of the linear temperature-dependent part to the specific heat is negligible. We intend to give detailed calculations in a separate paper.

VI. SUMMARY

(1) The lattice dynamics in thin film carbons are investigated in the long wavelength approximation by imposing appropriate boundary conditions on the sample surface.

(2) The Rayleigh wave, with a small damping constant and with polarization along the c axis, has a small sound velocity $v_R \sim 10^4$ cm/sec if C_{44} is small. The electron–Rayleigh-wave phonon interaction is obtained and the scattering rate of carriers is evaluated. Of particular interest for transport properties is the carrier relaxation time $\tau_R \sim 10^{-12}$ sec for a thin film with thickness $d < 100$ Å at $T \sim 1$ K. If the sample is assumed to be composed of an aggregation of many thin films and each film weakly couples elastically to the others, the present theory is applicable to a sample with bulk thickness. The electron–Rayleigh-wave interaction can explain the unusual temperature-dependent resistivity of PAN fibers heat treated to ~ 1300 °C.

(3) The Rayleigh-wave contribution can explain the linear temperature-dependent specific heat observed in some disordered carbons.

ACKNOWLEDGMENT

The author would like to express his sincere thanks to Professor M. S. Dresselhaus for her careful reading of this paper and for her stimulating discussions. This work was supported by the Air Force under AFOSR Contract No. F 49620-85-C-0147.

[1] K. Komatsu and T. Nagamiya, J. Phys. Soc. Jpn. **6**, 438 (1951); K. Komatsu, J. Phys. Soc. Jpn. **10**, 346 (1955).
[2] A. Yoshimori and Y. Kitano, J. Phys. Soc. Jpn. **11**, 352 (1956).
[3] J. A. Krumhansl and H. Brooks, J. Chem. Phys. **21**, 1663 (1963).
[4] R. Nicklow, N. Wakabayashi, and H. G. Smith, Phys. Rev. B **59**, 4951 (1972).
[5] E. S. Seldin and C. W. Nezbeda, J. Appl. Phys. **41**, 3389 (1970).
[6] R. Al-Jishi and G. Dresselhaus, Phys. Rev. B **26**, 4514 (1982).
[7] M. S. Dresselhaus and G. Dresselhaus, in *Intercalated Layer Materials*, edited by F. Levy (Reidel, Dordrecht, Holland, 1979), p. 423.
[8] K. Komatsu, J. Phys. Chem. Solids **25**, 704 (1964).
[9] B. J. C. van der Hoeven and P.H. Keesom, Phys. Rev. **130**, 1318 (1963).
[10] I. L. Spain, K. J. Volin, H. A. Goldberg, and I. L. Kalnin, Solid State Commun. **45**, 817 (1983).
[11] H. A. Goldberg, I. L. Kalnin, I. L. Spain, and K. J. Volnin, *Extended Abstracts of 16th Conference on Carbon, San Diego, 1983* (American Carbon Society, State College, PA, 1983), p. 281.
[12] S. Mrozowski, J. Low Temp. Phys. **35**, 231 (1979).
[13] L. D. Landau and E. M. Lifshitz, *Theory of Elasticity*, 2nd ed. (Pergamon, New York, 1970), Chap. III.
[14] B. T. Kelly, *Physics of Graphite* (Applied Science, London, 1981).
[15] K. Sugihara and H. Sato, J. Phys. Soc. Jpn. **18**, 332 (1963).
[16] S. Ono and K. Sugihara, J. Phys. Soc. Jpn. **21**, 866 (1966).
[17] K. Sugihara and M. S. Dresselhaus, *Extended Abstracts, Graphite Intercalation Compounds, 1986 Fall Meeting of the Materials Research Society*, edited by M. S. Dresselhaus, G. Dresselhaus, and S. A. Solin (Materials Research Society, Pittsburgh, PA, 1986), p. 135.
[18] P. Delhaes, P. de Kepper, and M. Uhlrich, Philos. Mag. **29**, 1301 (1974).
[19] P. Delhaes and Y. Hishiyama, Carbon **8**, 31 (1970).
[20] A. S. Vagh and S. Mrozowski, Carbon **13**, 301 (1975).
[21] P. H. Keesom and N. Pearlman, Phys. Rev. **99**, 1119 (1955).
[22] K. Kamiya, S. Mrozowki, and A. S. Vagh, Carbon **10**, 267 (1972).
[23] S. Mrozowski and A. S. Vagh, Carbon **14**, 211 (1976).